Particle Acceleration in High-Energy Astrophysical Plasmas: The interplay of Turbulence and Magnetic Reconnection

Luca Comisso and Lorenzo Sironi

Department of Astronomy, Columbia University
Columbia Astrophysics Laboratory, Columbia University

Multiscale Phenomena in Plasma Astrophysics

KITP, Santa Barbara, USA, October 10, 2019.

Astrophysical motivation

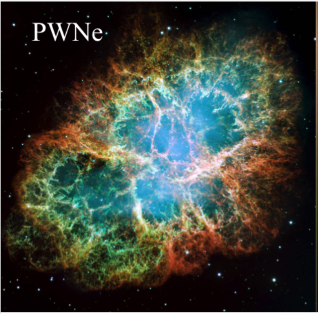

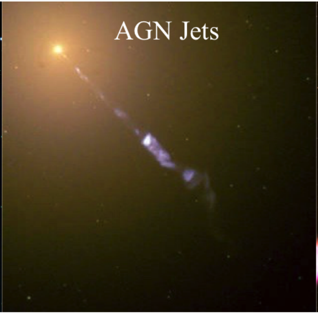

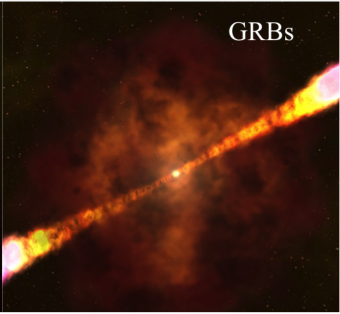

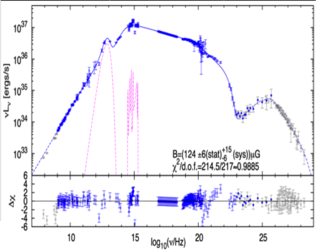

Meyer et al 2010

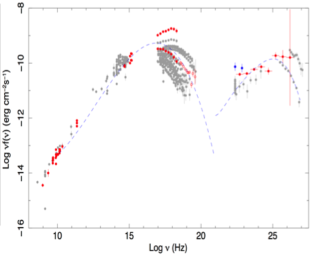

Abdo et al 2010

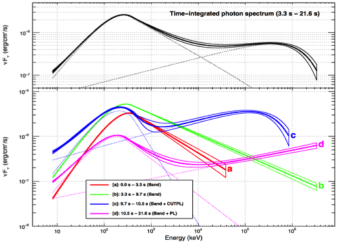

Ackermann et al 2011

Questions we want to address

- Is turbulence in magnetically-dominated plasmas an efficient source of nonthermal particles?

- If so, how does the nonthermal spectrum depend on the system parameters?

- Mechanisms of particle acceleration? Interplay with magnetic reconnection?

The results discussed in this talk can be found in:
Comisso & Sironi, PRL 2018 ; Comisso & Sironi, ApJ 2019

How can we tackle this problem?

- Understanding particle acceleration by plasma turbulence requires solving a complex, nonlinear multiscale problem

- An analytic treatment that solves the full initial value problem is practically unfeasible

  $\Rightarrow$ we must rely on numerical simulations of the underlying model equations

- The possible approaches essentially are:

  $\Rightarrow$ *test particle simulations*

  - with turbulent fields represented by prescribed fields
  - with turbulent fields obtained from MHD/fluid simulations

  $\Rightarrow$ *hybrid simulations* (kinetic ions and fluid electrons)

  $\Rightarrow$ *fully-kinetic simulations*

Our numerical method

- Fully-kinetic treatment:

  $\Rightarrow$ we solve the coupled Vlasov-Maxwell system of equations through the PIC method

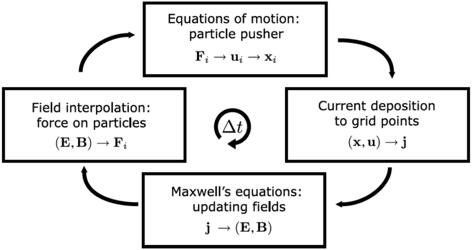

- PIC code TRISTAN-MP (Spitkovsky 2005)

- large-scale 2D (4100^2-65600^2 cells) and 3D (2460^3 cells) simulations ($\Rightarrow$ to cover both MHD and kinetic turbulence)

Turbulence setup

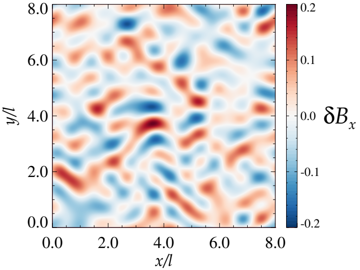

- Decaying turbulence
- mean magnetic field $\langle \boldsymbol{B} \rangle = B_0 \hat{\boldsymbol{z}}$
- turbulence develops from uncorrelated magnetic fluctuations δB_x and δB_y in Fourier harmonics
- energy-carrying scale: $l = 2\pi/k_f$

- Pair plasma in the magnetically-dominated regime

$$\sigma_0 = \frac{\delta B_{\mathrm{rms0}}^2}{4\pi w_0} \gg 1, \qquad \frac{\delta B_{\mathrm{rms0}}}{B_0} \sim 1, \qquad \theta = \frac{k_B T}{m_e c^2} \sim 1$$

with $w_0 = n m_e c^2 + n k_B T \left[\hat{\gamma}/(\hat{\gamma}-1)\right]$

Fully-developed turbulence state

2D simulation with $\sigma_0 = 10$, $\delta B_{\mathrm{rms}0}/B_0 = 1$, $L/d_{e0} = 1640$

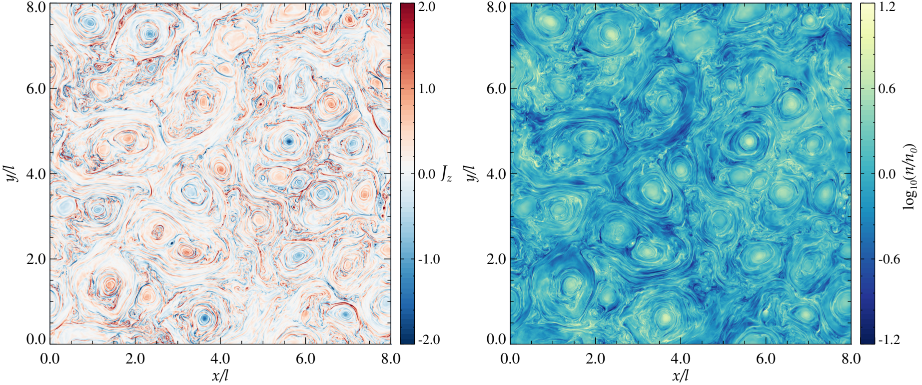

- Copious generation of current sheets and plasmoids

Fully-developed turbulence state

3D simulation with $\sigma_0 = 10$, $\delta B_{\mathrm{rms0}}/B_0 = 1$, $L/d_{e0} = 820$

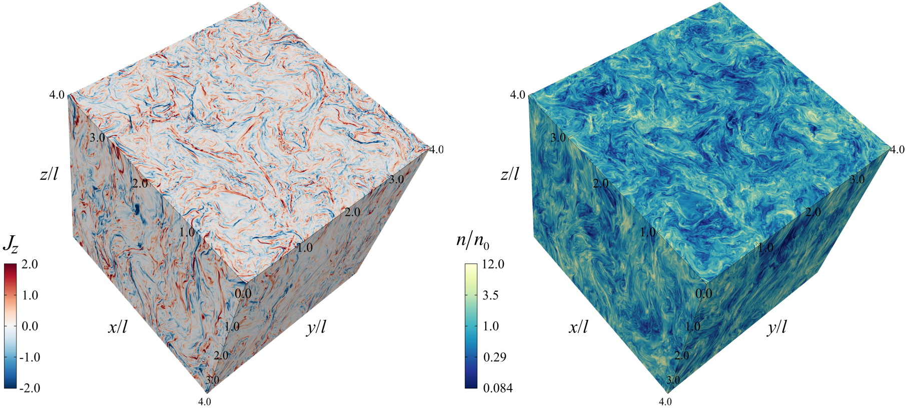

- Copious generation of current sheets and flux ropes

Fly-through J_z along the z-direction

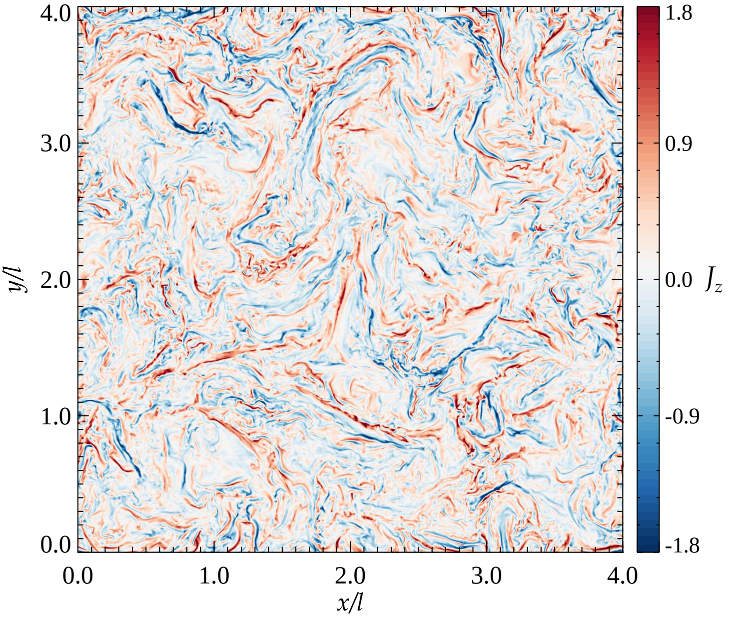

Turbulent cascade from MHD to kinetic scales

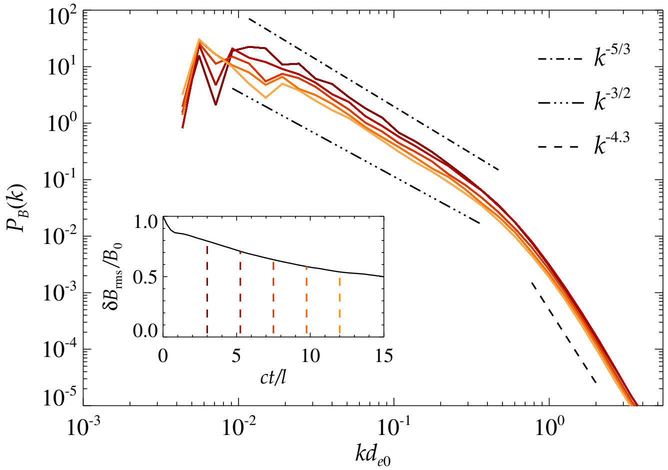

- Computational domain is large enough to capture both the MHD cascade at large scales and the kinetic cascade at small scales

Turbulent cascade from MHD to kinetic scales

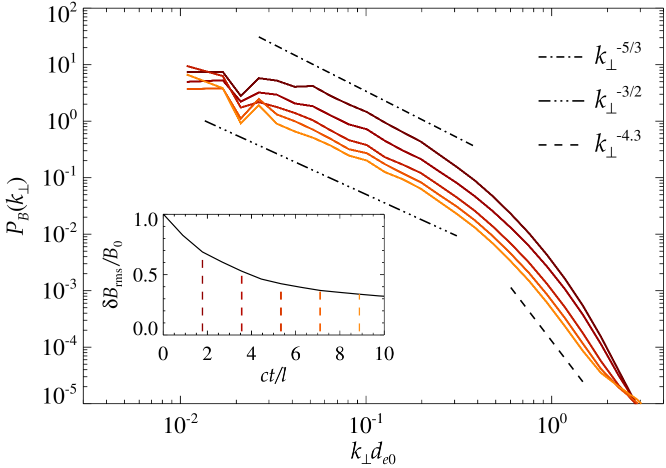

- Computational domain is large enough to capture both the MHD cascade at large scales and the kinetic cascade at small scales

Self-consistent development of nonthermal particles

2D simulation with $\sigma_0 = 10$, $\delta B_{\text{rms}0}/B_0 = 1$, $L/d_{e0} = 1640$

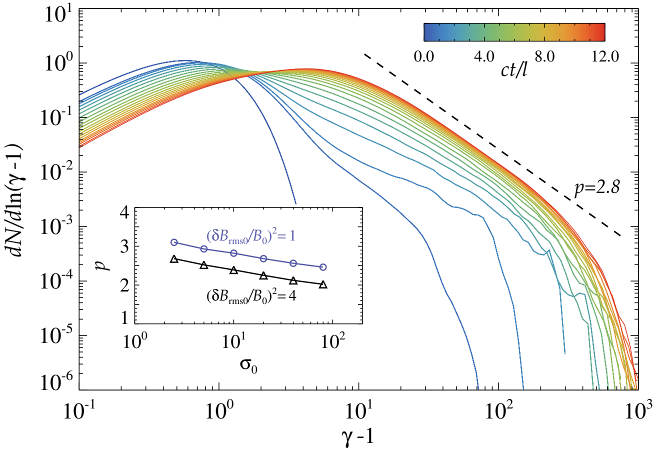

- A significant fraction of particles ($\sim 16\%$ for this simulation) populate the nonthermal-tail at late times (see also Zhdankin et al 2017/18, Nättilä 2019)

Different dimensionality, similar outcome?

3D simulation with $\sigma_0 = 10$, $\delta B_{\rm rms0}/B_0 = 1$, $L/d_{e0} = 820$

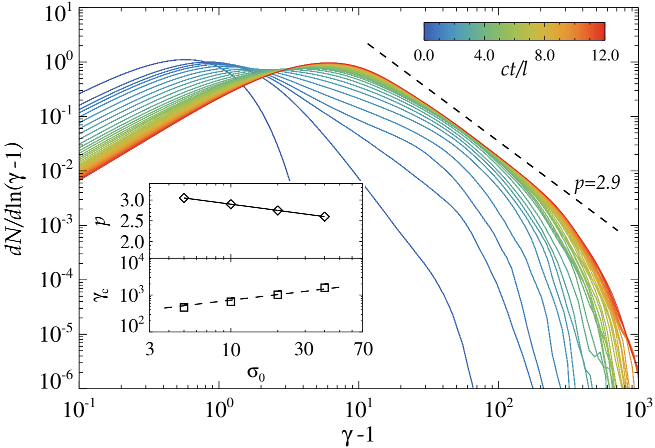

$$\gamma_{st} \sim \gamma_\sigma = \left(1 + \frac{\sigma_0}{2}\right)\gamma_{th0}\ , \qquad \gamma_c \sim e\sqrt{\langle B^2 \rangle}\frac{l}{mc^2} \sim \sqrt{\sigma_z}\gamma_{th0}(l/d_{e0})$$

Can we extrapolate our results to much larger systems?

2D simulations with $\sigma_0 = 10$, $\delta B_{\rm rms0}/B_0 = 1$

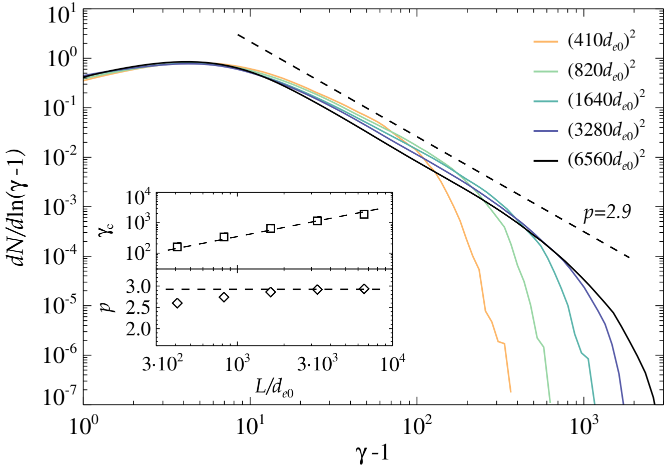

- The results are converged to $p =$ const and $\gamma_c \sim e\sqrt{\langle B^2\rangle} l/mc^2$.
  (see also Zhdankin et al 2018)

The power-law slope can become quite hard

2D simulations with $\sigma_0 = 40$, $L/d_{e0} = 3280$

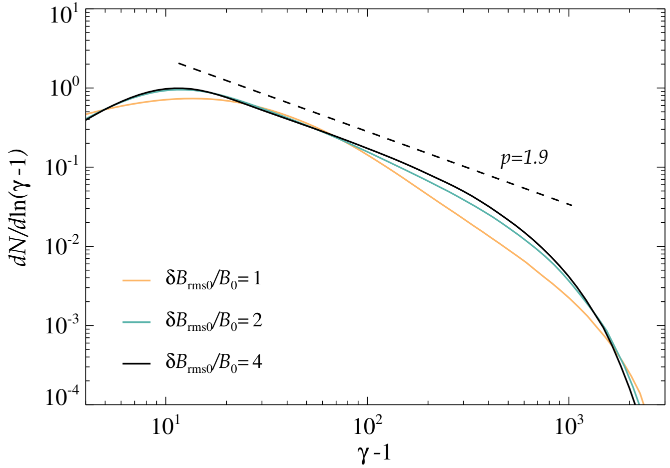

- For larger initial fluctuations $\delta B_{\rm rms0}/B_0$ ad magnetization σ_0, the power-law index decreases and can be $p < 2$.

Let's recap what we learned from PIC simulations

- The generation of a significant fraction ($\sim 15\% - 30\%$) of nonthermal particles is a generic by-product of magnetically-dominated plasma turbulence
- The cutoff Lorentz factor γ_c increases linearly with the energy containing scale of turbulence
- The slope p of the power law become harder for larger initial magnetization σ_0 and higher initial fluctuations $\delta B_{\mathrm{rms0}}/B_0$

but...

- We still need to understand the particle acceleration mechanism (i.e., the most interesting part starts now)

An instructive (1st) movie

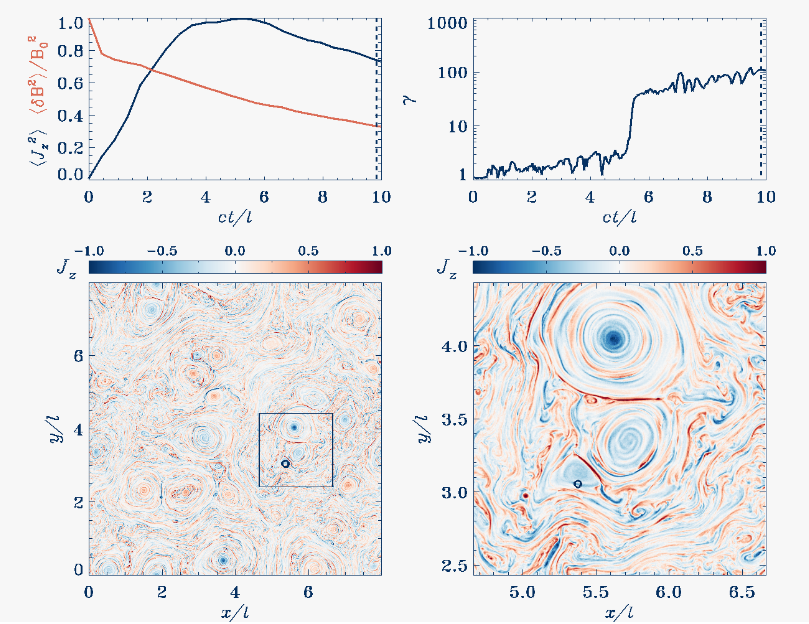

An instructive (2nd) movie

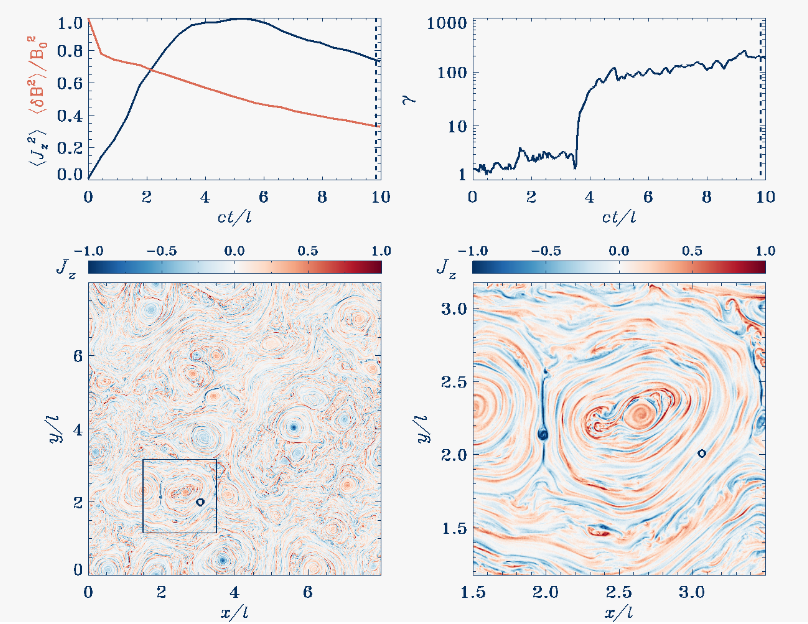

Particle Injection

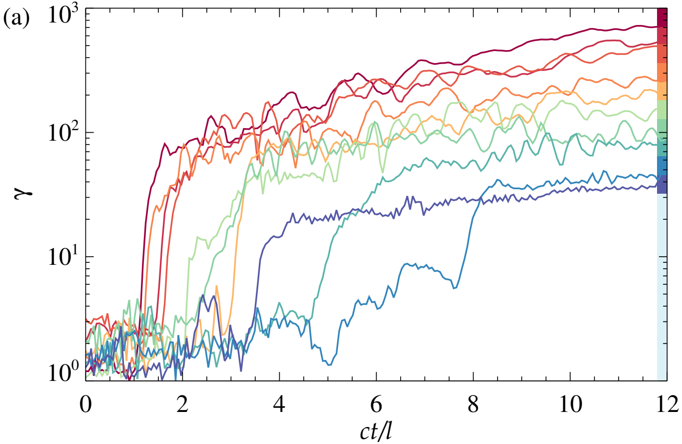

- The vast majority of the particles belonging to the nonthermail tail experience a sudden energy jump from $\gamma mc^2 \sim \gamma_{th} mc^2$ to $\gamma mc^2 \gg \gamma_{th} mc^2$

Statistics of the current density at injection

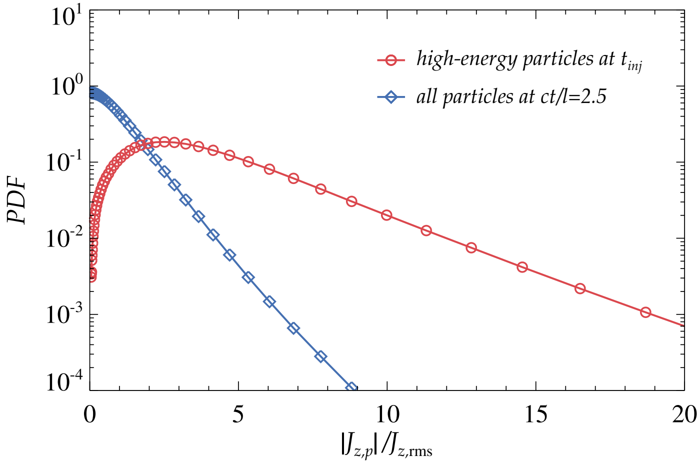

- Most of the high-energy particles reside at injection at $|J_{z,p}| \geq 2\, J_{z,\mathrm{rms}}$ (current sheets)

Most particle injection occurs at current sheets

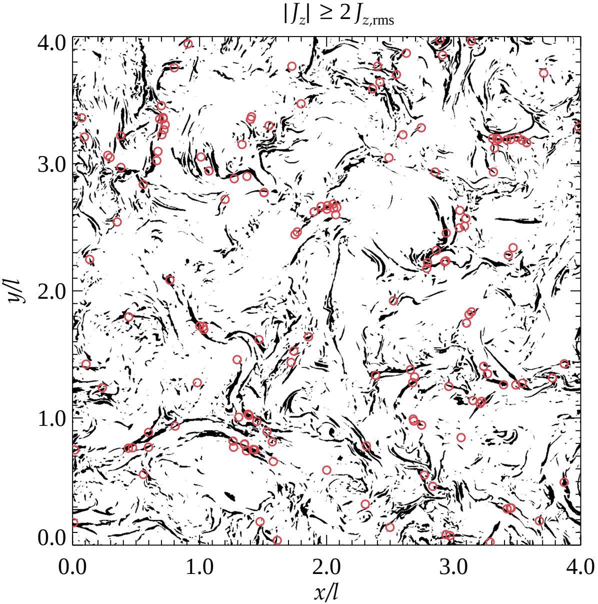

Reconnecting current sheets

- Collisionless tearing mode dispersion relation for a relativistic pair plasma:

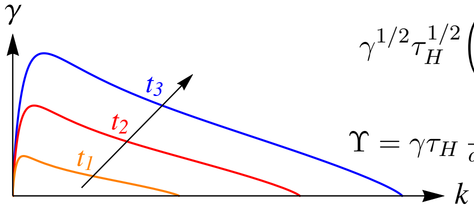

$$\gamma^{1/2}\tau_H^{1/2}\left(\frac{\lambda}{d_w}\right)^{3/2}\frac{\Gamma\left[(\Upsilon-1)/4\right]}{\Gamma\left[(\Upsilon+5)/4\right]} = -\frac{8}{\pi}\Delta'$$

$$\Upsilon = \gamma\tau_H\,\frac{\lambda}{d_w},\ \tau_H = \frac{1}{k_\xi v_{A\lambda}},\ d_w = \sqrt{\frac{mc^2}{4\pi n e^2}w}$$

- In a forming current sheet, the mode that becomes nonlinear in the shortest time disrupts the sheet when

$$\lambda_d \sim d_w^{2/3}\xi^{1/3}\left[\ln\left(\frac{1}{2\hat{\epsilon}^{1/2}}\left(\frac{d_w}{\xi}\right)^{\frac{4-\alpha}{6}}\right)\right]^{-1/3}$$

- $\lambda_d \gg d_w$ for outer-scale current sheets with $\xi \sim l \ggg d_w$

Reconnecting current sheets

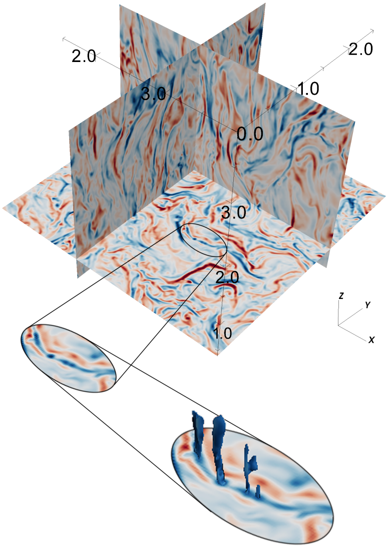

- A single reconnecting current sheet can "process" the upstream plasma up to a distance

$$\lambda_{R,j} = \beta_{R,j}\, c\, \tau_{\mathrm{nl},j} \sim \beta_{R,j}\, c \frac{\xi_j}{v_{A\lambda,j}}$$

- Thus, in one large-eddy turnover time, the reconnecting current sheets process a plasma volume

$$\mathcal{V}_R = \textstyle\sum_j \lambda_{R,j}\, \xi_j\, l_{\|,j} \sim \beta_R L^3$$

- β_R is the average reconnection rate. For fast reconnection $\beta_R = O(0.1)$
- Magnetic reconnection can process a large volume of plasma in few outer-scale eddy turnover times

Let's take a further look...

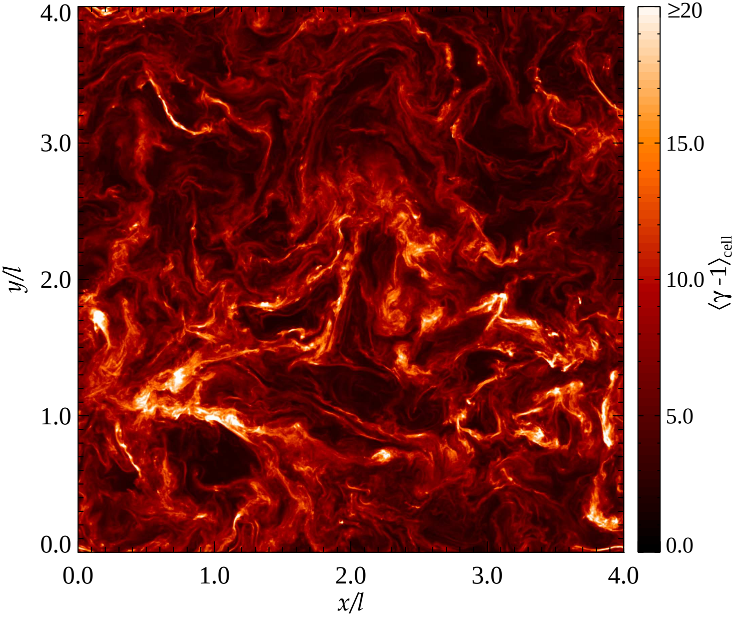

Particle energization: single particle

Energization history $[W_{\|,\perp}(t) = q \int_0^t \boldsymbol{E}_{\|,\perp}(t') \cdot \boldsymbol{v}(t')\, dt']$ for a typical high-energy particle

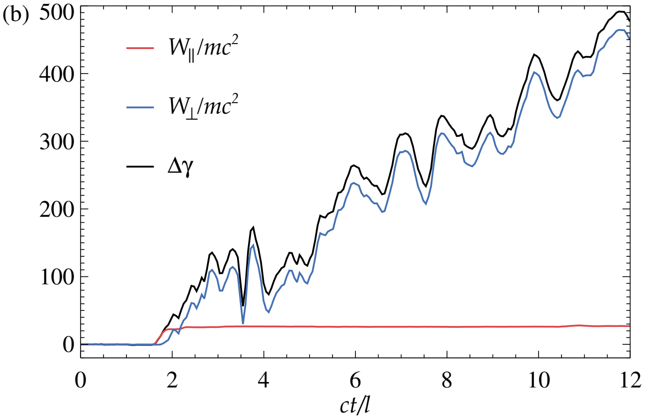

- The initial $\boldsymbol{v} \cdot \boldsymbol{E}_{\|}$ energization contributes only up to a certain energy. Then the $\boldsymbol{v} \cdot \boldsymbol{E}_{\perp}$ energization complete the work.

Same particle → slightly different plot

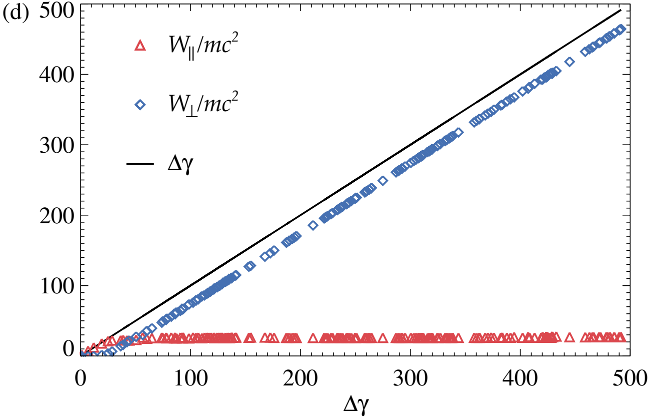

- But...how much "typical" is this typical high-energy particle?

Particle energization: particle statistics

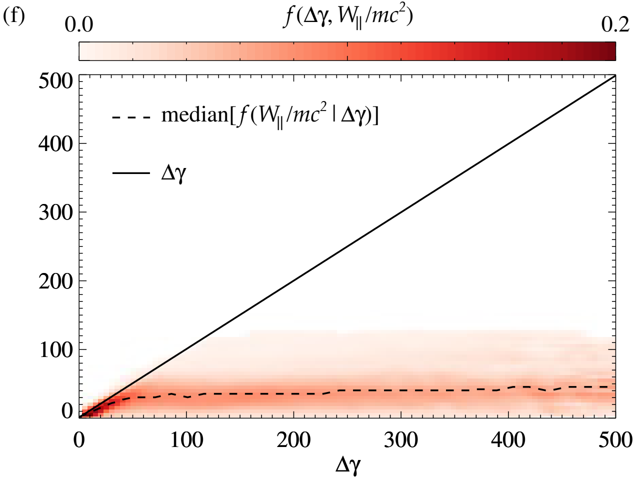

- The low $\Delta\gamma$-range is prevailed by the energization via $\boldsymbol{v} \cdot \boldsymbol{E}_{||}$
- $\boldsymbol{v} \cdot \boldsymbol{E}_{\perp}$ energization dominates the overall budget if $\Delta\gamma \gg \sigma_0 \gamma_{th0}$

Particle energization: particle statistics

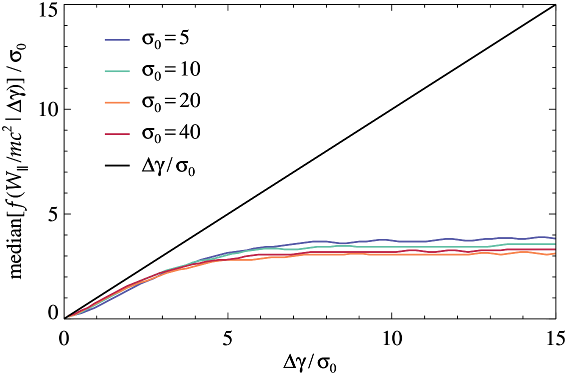

- The expected $\Delta\gamma$ governed by $\boldsymbol{E}_\parallel$ is

$$\Delta\gamma_{\rm inj} \sim W_\parallel/mc^2 \sim \kappa\sigma_0\gamma_{th0}\,, \quad \sigma_0 \gg 1 \tag{1}$$

- The length $l_{\rm inj}$ required to reach $\Delta\gamma_{\rm inj}$ is $l_{\rm inj} = \dfrac{\kappa}{\beta_R}\sqrt{\dfrac{\sigma}{w}}\,\gamma_{th} d_e$, which is always guaranteed for large enough systems, i.e. $l \gg l_{\rm inj}$.

What if we artificially remove $\boldsymbol{E}_{\|}$?

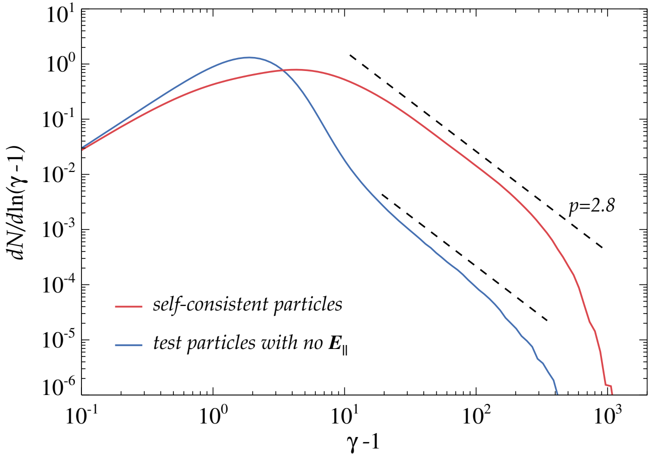

- The normalization drops by 2 orders of magnitude (only $\sim 0.2\%$ of the particles in the nonthermal tail)
  - On the other hand, the slope p is similar, as the high-energy particles "forget" their initial conditions

Particle energy diffusion

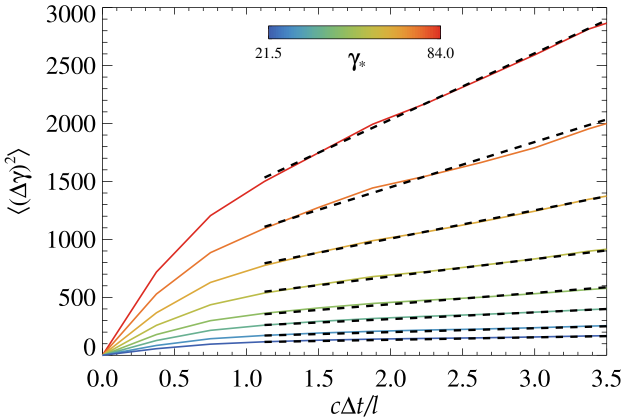

- From the particles evolution $\langle(\Delta\gamma)^2\rangle = \dfrac{1}{N_p}\sum_{n=1}^{N_p}\left(\gamma_n(t) - \gamma_n(t_*)\right)^2$
- Diffusive behavior in energy space, $\langle(\Delta\gamma)^2\rangle \propto \Delta t$ (see also Wong et al 19 for similar PIC results)

Diffusion coefficient in energy space

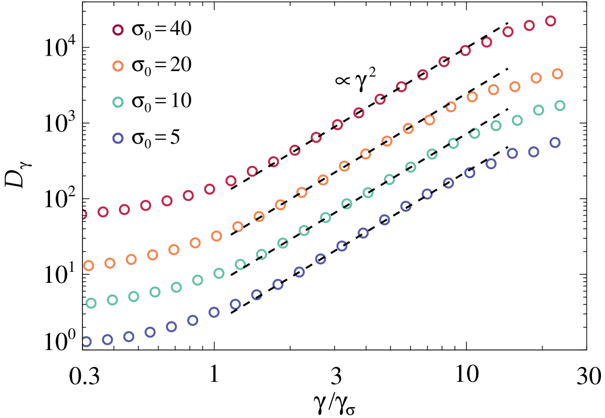

- The energy diffusion coefficient (in units of c/l) can be calculated as $D_\gamma = \dfrac{\langle(\Delta\gamma)^2\rangle}{2\Delta t}$ (see also Wong et al 19 for similar PIC results)
- The power-law tail of the particle spectrum starts at $\gamma/\gamma_\sigma \gtrsim 1$

Diffusion coefficient in energy space

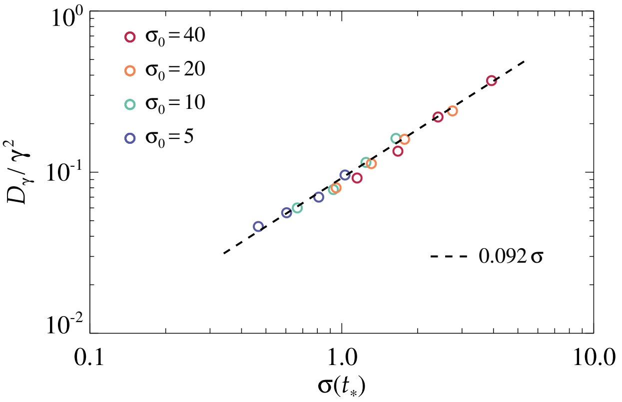

- The simulations are well fitted by $D_\gamma \sim 0.1\sigma \left(\frac{c}{l}\right) \gamma^2$
- Note that for a stochastic process akin to the original Fermi mechanism $D_\gamma = \frac{1}{3}\langle \gamma_V^2 \beta_V^2 \rangle \frac{c}{\lambda_{\rm mfp}} \gamma^2$ (e.g., Lemoine 2019)

Two-stage acceleration process

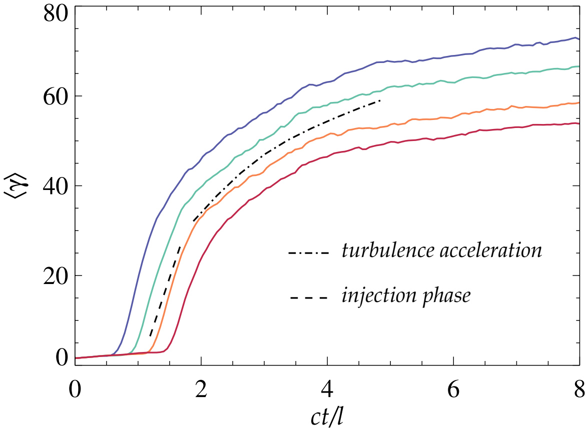

- Injection phase controlled by $E_{\|}$ gives $\dfrac{d\langle\gamma\rangle}{dt} = \dfrac{e}{mc}\beta_R \delta B_{\rm rms}$
- Acceleration controlled by D_γ gives $\dfrac{d\langle\gamma\rangle}{dt} = 4\kappa_{\rm stoc}\sigma\left(\dfrac{c}{l}\right)\gamma$

What happens to the particle distribution?

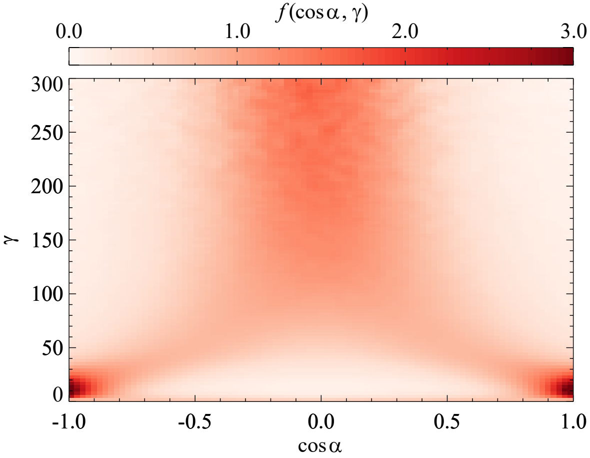

- Here: $\cos\alpha = \dfrac{\boldsymbol{v}\cdot\boldsymbol{B}}{|\boldsymbol{v}|\,|\boldsymbol{B}|}$, $\int_{-1}^{1} f\,(\cos\alpha,\gamma)\,d(\cos\alpha) = 1$
- The pitch-angle distribution develops distinguishing features at *low*, *intermediate*, and *high* values of γ

The anisotropy ranges are magnetization dependent

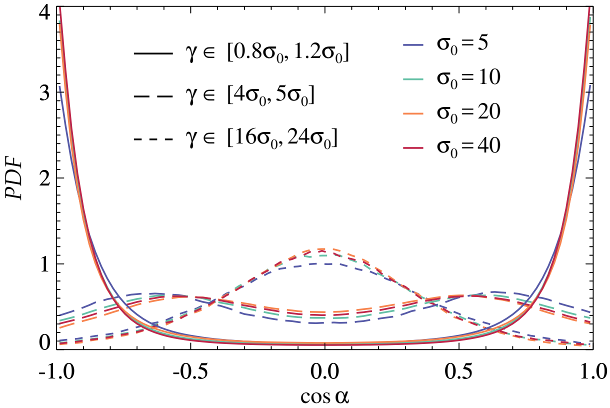

- $\gamma \sim (\sigma_0/2)\gamma_{th0} \Rightarrow$ particles $\boldsymbol{v}$ are strongly anti/aligned with $\boldsymbol{B}$
- $\gamma \sim 5(\sigma_0/2)\gamma_{th0} \Rightarrow$ distribution with minima at $\cos\alpha = \pm 1, 0$
- $\gamma \gg 5(\sigma_0/2)\gamma_{th0} \Rightarrow$ particles $\boldsymbol{v}$ are mostly perpendicular to $\boldsymbol{B}$

Anisotropy of the 4-velocity distribution

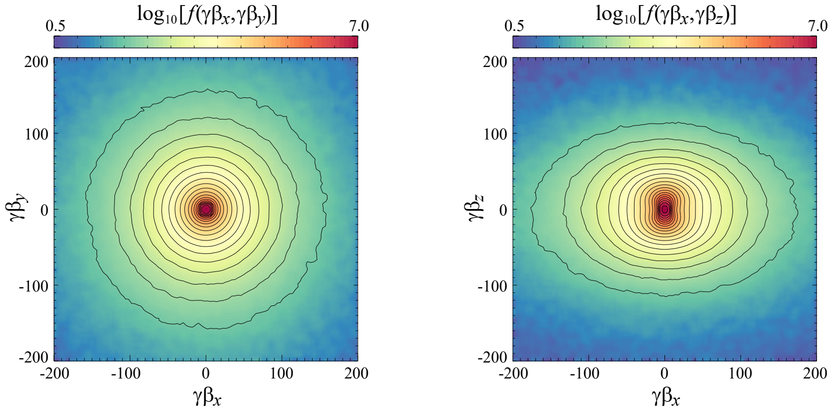

- The (domain-averaged) 4-velocity distribution is isotropic in the plane $\perp$ to $\boldsymbol{B}_0 = B_0\hat{\boldsymbol{z}}$, while for planes that contain $\boldsymbol{B}_0$:
  - core region elongated in the $\gamma\beta_z$ direction
  - elongated in the direction $\perp$ to $\boldsymbol{B}_0$ at high energies
  - double cone region at intermediate energies

Anisotropy of the 4-velocity distribution

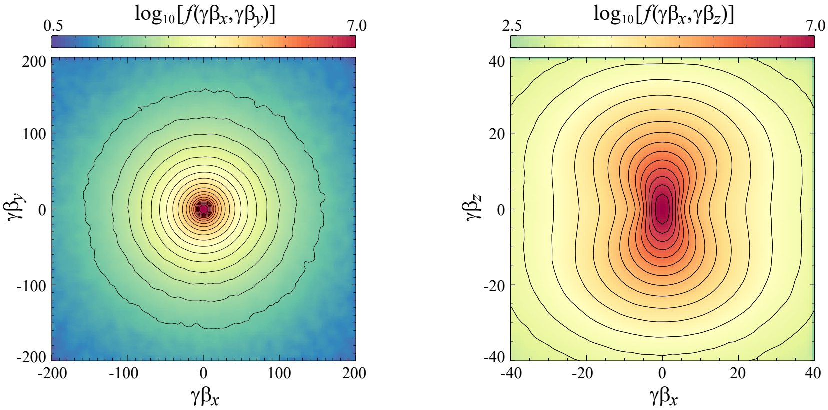

- The (domain-averaged) 4-velocity distribution is isotropic in the plane $\perp$ to $\boldsymbol{B}_0 = B_0 \hat{\boldsymbol{z}}$, while for planes that contain $\boldsymbol{B}_0$:
  - core region elongated in the $\gamma\beta_z$ direction
  - elongated in the direction $\perp$ to $\boldsymbol{B}_0$ at high energies
  - double cone region at intermediate energies

Summary

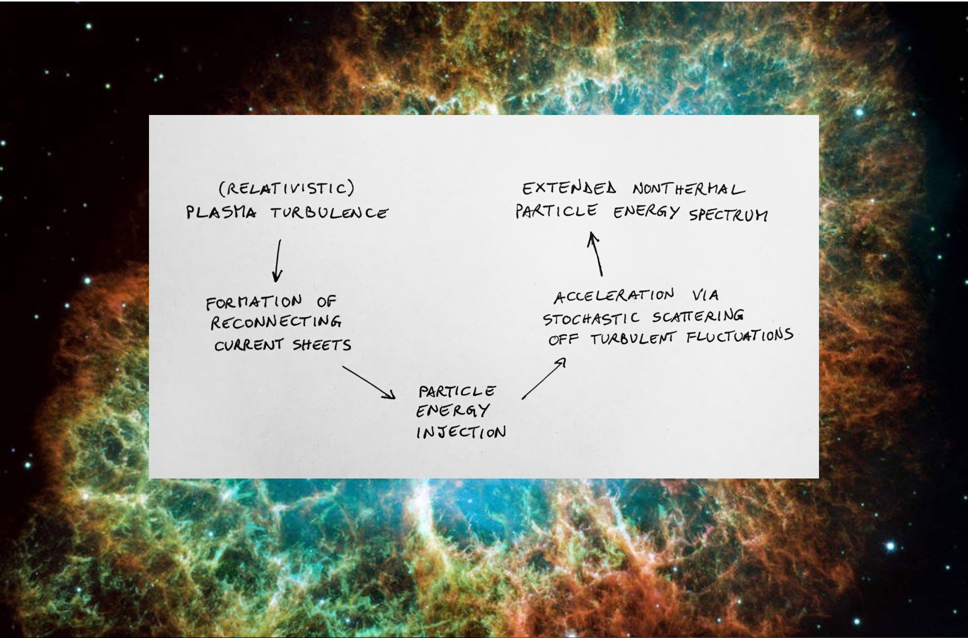
(RELATIVISTIC)
PLASMA TURBULENCE
FORMATION OF
RECONNECTING
CURRENT SHEETS
PARTICLE
ENERGY
INJECTION
ACCELERATION VIA
STOCHASTIC SCATTERING
OFF TURBULENT FLUCTUATIONS
EXTENDED NONTHERMAL
PARTICLE ENERGY SPECTRUM